



Early defects in translation elongation factor 1 α levels at excitatory synapses in α -synucleinopathy

Sonja Blumenstock^{1,2,8,9} · Maria Florencia Angelo^{3,4} · Finn Peters² · Mario M. Dorostkar¹ · Viktoria C. Ruf¹ · Manja Luckner⁵ · Sophie Crux^{2,8} · Lenka Slapakova¹ · Thomas Arzberger^{1,6,8} · Stéphane Claverol⁷ · Etienne Herzog^{3,4} · Jochen Herms^{1,2,8}

Received: 5 August 2019 / Revised: 14 August 2019 / Accepted: 15 August 2019 / Published online: 26 August 2019
© Springer-Verlag GmbH Germany, part of Springer Nature 2019

Abstract

Cognitive decline and dementia in neurodegenerative diseases are associated with synapse dysfunction and loss, which may precede neuron loss by several years. While misfolded and aggregated α -synuclein is recognized in the disease progression of synucleinopathies, the nature of glutamatergic synapse dysfunction and loss remains incompletely understood. Using fluorescence-activated synaptosome sorting (FASS), we enriched excitatory glutamatergic synaptosomes from mice overexpressing human alpha-synuclein (h- α S) and wild-type littermates to unprecedented purity. Subsequent label-free proteomic quantification revealed a set of proteins differentially expressed upon human alpha-synuclein overexpression. These include overrepresented proteins involved in the synaptic vesicle cycle, ER–Golgi trafficking, metabolism and cytoskeleton. Unexpectedly, we found and validated a steep reduction of eukaryotic translation elongation factor 1 alpha (eEF1A1) levels in excitatory synapses at early stages of h- α S mouse model pathology. While eEF1A1 reduction correlated with the loss of postsynapses, its immunoreactivity was found on both sides of excitatory synapses. Moreover, we observed a reduction in eEF1A1 immunoreactivity in the cingulate gyrus neuropil of patients with Lewy body disease along with a reduction in PSD95 levels. Altogether, our results suggest a link between structural impairments underlying cognitive decline in neurodegenerative disorders and local synaptic defects. eEF1A1 may therefore represent a limiting factor to synapse maintenance.

Keywords Alpha-synuclein · Elongation factor 1 alpha · Synapse · Proteomics · Lewy body dementia · FASS

Etienne Herzog and Jochen Herms contributed equally to this work.

Electronic supplementary material The online version of this article (<https://doi.org/10.1007/s00401-019-02063-3>) contains supplementary material, which is available to authorized users.

✉ Etienne Herzog
etienne.herzog@u-bordeaux.fr

✉ Jochen Herms
jochen.herms@med.uni-muenchen.de

¹ Center for Neuropathology and Prion Research, Ludwig-Maximilians University, Munich, Germany

² German Center for Neurodegenerative Diseases (DZNE), Munich, Germany

³ Université de Bordeaux, Interdisciplinary Institute for Neuroscience, UMR5297, 33000 Bordeaux, France

⁴ CNRS, Interdisciplinary Institute for Neuroscience, UMR5297, 33000 Bordeaux, France

Introduction

Since the description of alpha-synuclein (α -syn) as the major constituent of Lewy bodies [70], this protein has been in the focus for understanding the etiology of a group of diseases called synucleinopathies. Parkinson's disease (PD)

⁵ Department of Biology I, Biozentrum Ludwig-Maximilians University, Munich, Germany

⁶ Department of Psychiatry and Psychotherapy, University Hospital, Ludwig-Maximilians University, Munich, Germany

⁷ Plateforme Proteome, Centre Génomique Fonctionnelle de Bordeaux, Université de Bordeaux, Bordeaux, France

⁸ Munich Cluster of Systems Neurology (SyNergy), Munich, Germany

⁹ Present Address: Department Molecules-Signaling-Development, Max Planck Institute of Neurobiology, Martinsried, Germany

is the most prominent member of this group which further includes Parkinson's disease dementia (PDD), dementia with Lewy bodies (DLB), multiple system atrophy (MSA) and some less well-characterized neuroaxonal dystrophies [80].

In neurons, α -syn is a component of synaptic vesicles and has been described as unfolded when soluble in the cytoplasm and forming α -helices when binding to curved membranes [6] and lipid rafts [5, 24, 27, 29]. α -syn influences synaptic vesicle clustering [24, 31, 67], exocytosis [48, 59, 67], endocytosis [81] and microtubule dynamics [15]. Nevertheless, the molecular mechanism responsible for the presynaptic (dys-)functions of α -syn remains poorly understood and the triggers for α -syn accumulation in synucleinopathies are not precisely known.

In a previous study, we have shown that the excess of α -syn causes destabilization and loss of dendritic spines in the mouse neocortex. Mice overexpressing α -syn under the PDGF β promoter show high levels of cortical α -syn [2, 52] and spine loss months before any behavioral impairment becomes apparent [8]. Yet, the molecular changes underlying the observed synapse loss remained unknown. Therefore, we embarked on an unbiased mass spectrometry approach to analyze the relative protein composition between excitatory synapses of PDGF-h- α S and control mouse forebrains.

Due to the enormous complexity of brain tissue proteome [26, 40, 68] and the synaptic localization of α -syn [29, 49], a sample preparation that aims to reduce complexity and to remove extra-synaptic peptides is mandatory. To that end, subcellular fractionation of intact synaptic compartments—termed synaptosomes—has been used [21, 34, 79]. Yet this type of samples still suffer from the presence of a significant fraction of extra-synaptic material and all types of synapses regardless of their neurochemical nature [66]. We recently developed the fluorescence-activated synaptosome sorting (FASS) which allows the separation of specific synaptic subpopulations using a genetically encoded fluorescence reporter and a cell sorter [7, 50]. FASS purification of excitatory synaptosomes labeled with the vesicular glutamate transporter VGLUT1^{VENUS} [39] depleted several hundreds of proteins compared to classical sucrose synaptosomes and thus permitted the identification of new synaptic players [7].

In the present work, we applied FASS purification of VGLUT1^{venus} excitatory synapses to PDGF-h- α S and control littermates. Label-free quantitative analysis of their protein composition revealed the upregulation of 40 proteins and the downregulation of 2 proteins. Interestingly, the multi-function translation elongation factor eEF1A1 displayed a massive drop in expression upon α -syn overexpression [1, 53]. We thus further investigated the behavior of this marker in our mouse model and post-mortem tissue from patients with Lewy body disease (LBD). Our results point to an early molecular event involved in α -syn-mediated

synapse dysfunction and loss which are relevant in human α -synucleinopathies.

Materials and methods

Animals

PDGF-h- α S transgenic mice were obtained from QPS Austria Neuropharmacology (Grambach, Austria) and bred on a C57Bl/6 background [52]. The generation and characterization of the VGLUT1^{VENUS} knock-in mouse line were previously described [39]. C57Bl6 wild-type and Thy1-eGFP transgenic mice (GFP-M) were obtained from Jackson Laboratory (Bar Harbor, ME, USA). PDGF-h- α S \times VGLUT1^{VENUS} (termed h- α S in this paper) and PDGF-h- α S \times GFP-M lines were created by interbreeding. All animals were housed in groups under pathogen-free conditions and bred in the animal housing facility at the Center for Neuropathology and Prion Research of the Ludwig-Maximilians-University Munich, with food and water provided ad libitum (21 ± 2 °C, at 12/12-h light/dark cycle). Breeding and experimental procedures followed the European guide for the care and use of laboratory animals and the Ethical Review Board of the Government of Upper Bavaria (Az. 55.2-1-54-2532-204-2014) and the current laws of France. All data are reported according to the ARRIVE criteria [45].

Post-mortem tissue samples

Post-mortem human tissue samples were obtained from the Neurobiobank Munich. All donors or their families provided written informed consent for brain donation. Samples were collected in accordance with Institutional Review Board protocols approved by the local ethics committee (#345-13). Ethics approval for the procedures of this study was granted (#17-722). All procedures of this study were in accordance with the 1964 Helsinki Declaration and its later amendments or comparable ethical standards. Studies were performed using tissue from patients with neuropathologically confirmed LBD [77] and age-matched controls. Samples from LBD patients were at Braak stages 3/4 (termed 'mid-stage') and stages 5/6 (termed 'late-stage') [9] (Supplementary Table S4, online resource). For immunohistochemistry, formalin-fixed and paraffin-embedded tissue of the anterior cingulate gyrus was used (LBD: $n = 18$; ctrl: $n = 9$). For Western blot, frozen tissue of the anterior cingulate gyrus was homogenized in ten volumes of lysis buffer [Tris-buffered saline containing 2% SDS and 1 \times Complete protease inhibitor mixture (Roche)] using a OMNI TH homogenizer and centrifuged at 17,000g for 1 h at 4 °C. The resulting supernatants were used for Western blotting (LBD: $n = 6$, late-stage; ctrl: $n = 5$).

Preparation of S-synaptosomes and FACS instrumentation

For the enrichment of glutamatergic synaptosomes and the concurrent study of proteomic changes due to excess α -syn, we used mice carrying the VGLUT1^{VENUS} knock-in Ref. [39] and the PDGF-h- α S transgene [52] at 12–13 weeks of age. Littermates negative for h- α S were used as controls. The S-synaptosome preparation was adapted from a protocol previously described [7, 79]. Sample size for FASS was 12 animals (6 WT, 2 \times 3 PDGF-h- α S \times VGLUT1^{VENUS}, littermates, mixed gender, 12 weeks old). Details on synaptosome preparation and FASS gating strategy were described previously [7, 50] and additionally can be found in the online supplementary material.

Fluorescence-activated synaptosome sorting (FASS) and protein recovery

Fresh S-synaptosomes were diluted, kept cold and protected from light. Directly before sorting, incubation of synaptosomes with the lipophilic styryl dye FM4-64 (1 μ g/ μ l) provided bulk red labeling of membranes. Samples were analyzed and sorted at event rates of 18,000–22,000 evt/s until approximately 80×10^6 particles had been collected. To test the quality of sorted samples (FASS synaptosomes), they were reanalyzed by flow cytometry with identical instrument setting. Before proteomic analysis, FASS synaptosomes were concentrated on polycarbonate filters with a pore size of 0.1 μ m using a custom-built vacuum concentrator. Proteins were recovered with 70 μ l of SDS sample buffer and sample concentration was determined through SDS-PAGE and regular silver staining.

SDS-PAGE and Western blotting

The primary antibodies used in this study are listed in Supplementary Table S1 (online resource). SDS-PAGE using 4–20% Mini-PROTEAN[®] TGX Stain-Free[™] gels (Bio-Rad) were carried out according to the manufacturer's recommendations, while Western blotting was performed according to standard procedures. We used fluorophore coupled secondary antibodies (Li-Cor, 1:20,000) and visualized signals with an Odyssey[®] Classic scanner and Image Studio[™] software. Quantification of bands was performed in ImageJ (National Institutes of Health) and their intensity was normalized to the intensity of bands in the entire lane, using Bio-Rad's stain-free blot technology, ImageLab software (Bio-Rad) and a ChemiDoc[™] system.

Immunofluorescence

1 ml (correlating to $\sim 10^6$ particles) of diluted FASS synaptosomes were added on top of a 12 mm diameter gelatinized cover slip and centrifuged for 34 min at 6800g. FASS synaptosomes were fixed with 4% paraformaldehyde for 20 min, washed and stored in PBS. Primary antibody incubation was performed overnight at 4 °C, followed by secondary antibody incubation for 1 h at room temperature. For mounting on glass coverslips, VECTASHIELD[®] Mounting Medium (Vector Laboratories) was used. For immunofluorescence in free-floating sections, mice were transcardially perfused with 1 \times phosphate-buffered saline (PBS) and 4% paraformaldehyde under deep ketamine/xylazine anesthesia. Slice preparation and staining were performed as previously described [8].

Immunohistochemistry

Immunohistochemistry (IHC) was performed on formalin-fixed, paraffin-embedded tissue which was sectioned (4 μ m per section), deparaffinized, and rehydrated. Immunohistochemical staining was done using primary eEF1A1 antibody, UltraView DAB Detection Kit and a Ventana BenchMark ULTRA staining instrument (Roche) according to the manufacturer's specifications. The Ventana staining procedure included pretreatment with Cell Conditioner 1 (pH 6) for 56 min, followed by incubation with 1:1000 diluted eEF1A1 antibody at room temperature for 32 min and detection with UltraView DAB (Roche). Counterstaining with hematoxylin was performed prior to dehydration and mounting. For α -syn staining, the same protocol was adapted to use 36 min of pretreatment and 1:200 (pS129) or 1:2000 (α -syn42) diluted α -syn antibody.

Light microscopy

Confocal imaging of FASS synaptosomes was performed on an LSM 780 (Zeiss) equipped with a 63 \times /1.40 oil immersion objective. Laser wavelengths used for excitation and collection range of emitted signals were as follows: Alexa488/VGLUT1—488 nm/—585 nm; Alexa594—561 nm/585–743 nm; Alexa647—633 nm/638–755 nm. For imaging FASS synaptosomes, 16-bit data stacks of 2048 \times 2048 pixels were acquired from five different fields of view on the cover slip (lateral resolution 0.082 μ m/pixel, axial resolution 0.3 μ m/pixel). Stimulated emission depletion (STED) microscopy images were acquired on a Leica SP8-3XSTED microscope equipped with a 100 \times /1.40 oil immersion objective. Laser wavelengths used for excitation and depletion were as follows: Alexa488/VGLUT1—488 nm/670 nm; Alexa594/eEF1A—594 nm/670 nm. Pixel size was 22 nm, bit depth was set to 8 bits and several frames

were accumulated. Immunostained free-floating mouse brain sections were imaged accordingly: 16 bit, 1024 × 1024, lateral resolution 0.044 μm/pixel, axial resolution 0.2 μm/pixel. Confocal imaging of apical tuft dendrites in h-αS × GFP-M mice were performed as previously described [8]. DAB-stained immunohistochemical samples of human brain tissue were digitized on an Olympus BX41 microscope equipped with an Olympus SC30 digital camera using a 40× objective.

Electron microscopy

Transmission electron microscopy (TEM) was performed in the somatosensory cortex of h-αS and control mice ($n = 4$ per group). Detailed description of sample preparation and electron microscope settings can be found in the supplementary material.

Image processing and analysis

Analysis of spine density was performed on deconvoluted (AutoQuantX3, Media Cybernetics) confocal image stacks as previously described [8]. To quantify the immunofluorescence and VGLUT1^{VENUS} signal of individual FASS synaptosomes, custom-written MATLAB cluster analysis was applied. VGLUT1^{VENUS} positive synaptosomes were detected in 3D by applying the 80th percentile as minimal threshold. To separate contacting synaptosomes, the data were segmented morphologically by calculating the distance transformation, followed by watershed segmentation along minimal distance ridges. Only structures with a volume > 0.15 μm³ were counted as synaptosomes. The volume of each synaptosome was refined to correct for photon scattering. For this, the half-width VGLUT1^{VENUS} intensity was calculated and was used as a minimal threshold for the final dimension. The mean and summed VGLUT1^{VENUS} fluorescence signal and the immunofluorescence signal were calculated for the center plane of each synaptosome. In the case of postsynaptic proteins, the immunofluorescence commonly appears somewhat off the synaptosome. Therefore, the mean and summed immune signal were derived from contacting immunopositive structures. All images were recorded with identical laser power and microscope settings on the same day. Due to the thin sample size of 1 μm (diameter of single synaptosome), photon aberration only marginally deteriorates the signal intensity. Thus, detected fluorescence intensity constitutes a quantitative measure of the amount of labeled protein per synaptosome. Detection and quantification of eEF1A1-, VGLUT1- and PSD95-positive structures in mouse brain tissue were performed using Imaris v.7.7.2 (Bitplane Inc.) software with the spot detection algorithm [*XY* diameter: 0.5 μm (PSD95) or 0.7 μm (eEF1A1/VGLUT1); *Z* diameter: 1.4 μm]. Background subtraction was enabled and region growing type was set to

local contrast with a manual threshold of 30 defined for all datasets. Spots were filtered for volume > 0.01 μm². The data were compiled in MATLAB using ImarisXT interface. Color images from IHC stainings were color deconvoluted and converted to grayscale using ImageJ. Of the resulting image, the average intensity was calculated using inverted LUT, so that the lower values represent weaker immunosignal. TEM micrographs were analyzed with ImageJ, to measure the presynaptic area, length of postsynaptic density (PSD) and the number of synaptic vesicles (SV) to calculate vesicle density. For quantification of DAB staining intensity in neurons, cell bodies were detected semi-automatically using CellProfiler 3.0 [14].

Proteomics

Sample preparation and nanoliquid chromatography tandem mass spectrometry (nano LCMS/MS) as well as label-free quantitative data analysis and results processing are described in detail in the supplementary material.

Proteomics data archival

The mass spectrometry proteomics data have been deposited to the ProteomeXchange Consortium (<https://www.proteomecentral.proteomexchange.org>) via the PRIDE partner repository [76] with the dataset identifier PXD006812.

Bioinformatics

Gene ontology term and KEGG pathway analyses were done using DAVID Bioinformatics Resources 6.8, National Institute of Allergy and Infectious Diseases (NIAID), NIH [42, 43].

Statistics

The sample size of animals was calculated based on the experience from our previous work [7, 8]. Sample sizes of human material were based on tissue availability. Graphs were created and statistics were calculated in Prism v 7.04 (GraphPad Software, San Diego, CA, USA). For assessment of inter-group differences at single time points, Student's *t* test (unpaired, two-sided) was applied. Normal distribution was assumed according to the central limit theorem, as spine densities and immunofluorescence of FASS synaptosomes were calculated as the mean of means for every mouse. For *t* tests, the variance between groups was tested (*F* test) and not found to be significantly different. For comparing cumulative distributions, Kolmogorov–Smirnov test (KS test) was used. Data are expressed as mean ± s.e.m., with $p = 0.05$ as

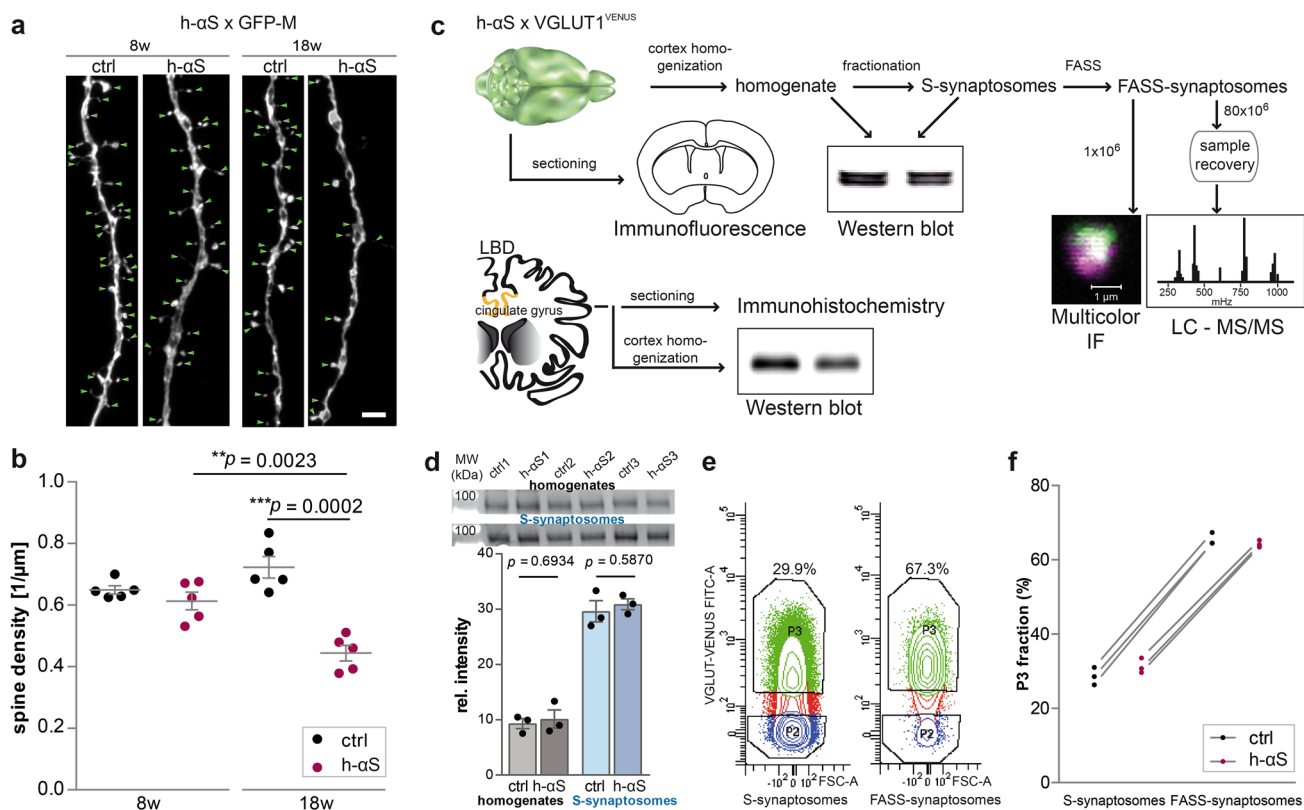


Fig. 1 Spine loss in PDGF-h- α S mice is the scientific background for FASS. **a** Exemplary confocal images of apical tuft dendrites with spines (green arrowheads) in the somatosensory cortex of h- α S x GFP-M mice. **b** Age-dependent spine loss in young adult h- α S mice occurs between 8 and 18 weeks of age. $n = 5$ mice per group, mean with s.e.m., Student's t test; ** $p < 0.01$, *** $p < 0.001$; scale bar = 5 μ m. **c** FASS workflow; synaptosomes were obtained from 12-week-old h- α S x VGLUT1^{VENUS} mice and purified using

FASS. Validation was performed on mouse and human brain tissue. **d** Western blot shows no differential expression of endogenous VGLUT1^{VENUS} levels in control and h- α S mice. **e** Sub-gating of particles according to their size and VGLUT1^{VENUS} fluorescence during FASS. Fraction P3 represents VGLUT1^{VENUS} positive events. **f** Independent FASS experiments from individual mice show comparable enrichment in VGLUT1^{VENUS} particles

significance threshold (* $p < 0.05$; ** $p < 0.01$; *** $p < 0.001$; **** $p < 0.0001$).

Results

Screening for proteins in VGLUT1-containing synapses by FASS

Our previous work showed that mice overexpressing human α -syn (PDGF-h- α S mice) progressively lose dendritic spines of excitatory cortical neurons [8]. Confocal imaging and analysis of apical tuft dendrites from layer V somatosensory cortical neurons in PDGF-h- α S x GFP-M mice (Fig. 1a) shows that dendritic spine density is not significantly different in mice aged 8 weeks. However, at 18 weeks of age, a reduction of spine density is present in h- α S mice, which agrees with our previous finding that spine loss starts to occur in an age-dependent manner at

around 12 weeks in these mice (Fig. 1b) [8]. Using this observation as a basis, we set out to investigate which changes in the protein composition of glutamatergic synapses might contribute to this phenotype.

The experimental workflow including synaptosome purification using FASS and validation using Western blot, immunofluorescence and immunohistochemistry of mouse and human brain tissue is illustrated in Fig. 1c. During the FASS procedure, 80×10^6 FASS synaptosomes were collected from each mouse sample for proteomic analysis. Additional 1×10^6 FASS synaptosomes were sedimented onto glass coverslips for immunofluorescence imaging (Fig. 1c). Endogenous VGLUT1^{VENUS} expression in homogenates and S-synaptosomes of the mice used for FASS was found to be not significantly different (Fig. 1d). Before sorting, S-synaptosome preparations contained ~30% VGLUT1^{VENUS} fluorescent particles eligible for sorting (ctrl: $28.7 \pm 2.35\%$; α S: $31.6 \pm 1.98\%$). After FASS sorting, the fraction of VGLUT1^{VENUS} positive particles increased

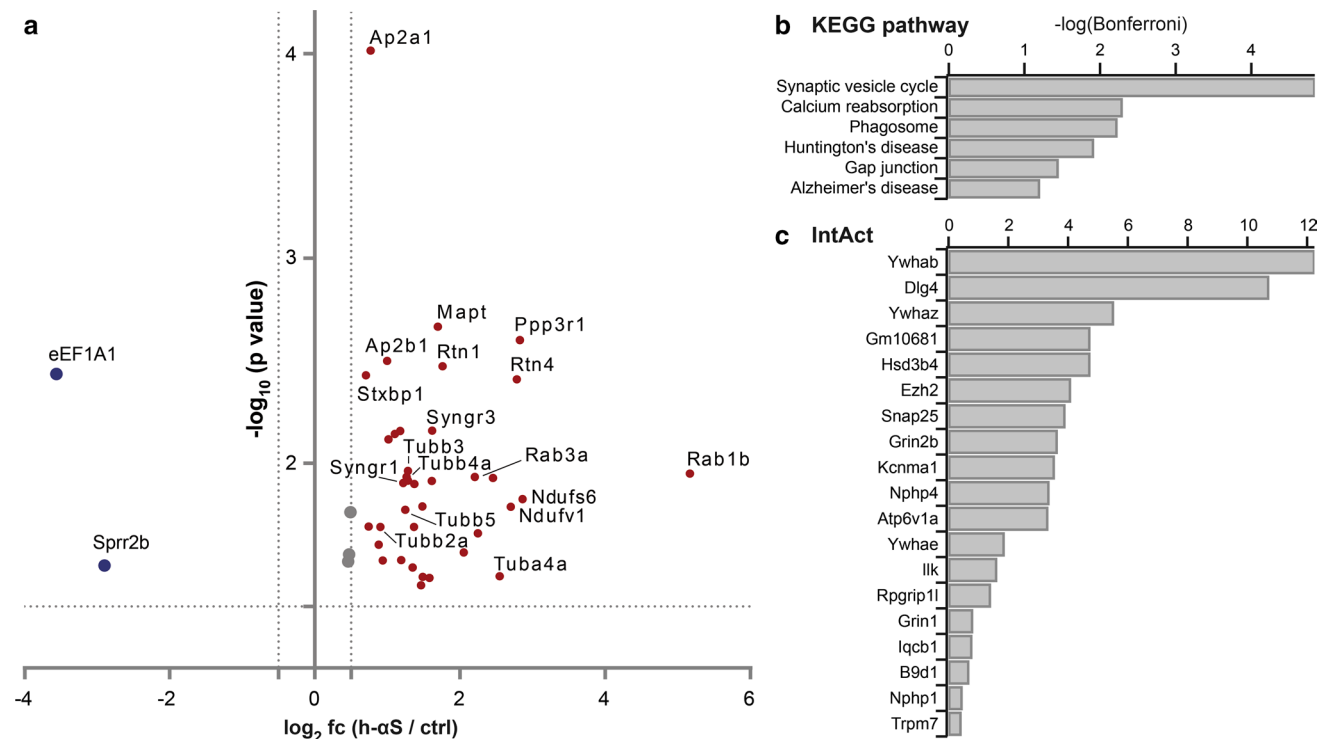


Fig. 2 Proteomic MS data reveals a set of 42 proteins with significantly different abundance in h- α S synaptosomes. **a** Graphic representation of protein hits according to \log_2 (fold change) and $-\log_{10}(p \text{ value})$. Gene names: Ap2a1/-b1: AP-2 complex subunit alpha-1/-beta1; eEF1A1: eukaryotic elongation factor 1 alpha-1; Mapt: microtubule-associated protein tau; Ppp3r1: calcineurin subunit B; Ndufs6: NADH dehydrogenase iron-sulfur protein 6; Nufv1: NADH dehydrogenase flavoprotein1; Rab1B/-3A: Ras-related protein

Rab-1B/-3A; Rtn 1/-4: Reticulon 1/-4; Sprr2b: small proline-rich protein 2B; Syng3: synaptogyrin 3; Stxbp1: syntaxin-binding protein 1 (Munc18-1); Tuba4a: tubulin alpha-4A; Tubb2a/-3/-4a/-5: tubulin beta-2A/-3/-4A/5. **b** KEGG pathway enrichment highlights the involvement of related cellular and disease-related protein pathways. **c** IntAct database analysis for the determination of the interacting proteomic network. The majority of proteins listed have eEF1A1 as interacting partner (see Supplementary Table S3, online resource)

to ~65% (ctrl: $65.9 \pm 1.44\%$; α S: $64.4 \pm 0.94\%$) (Fig. 1e). The enrichment in VGLUT1^{VENUS} fluorescent particles was comparable across all samples (Fig. 1f).

To systematically assess differences in protein composition of synapses in α S animals versus controls, we used mass spectrometry (MS)-based protein identification and label-free quantification. Samples ($n=3$ mice per group) were separated by one-dimensional SDS-PAGE, tryptically digested in the gel and analyzed by nano LC-MS/MS followed by protein database search using SEQUEST as a search engine. About 1200 protein groups were identified and quantified by label-free mass spectrometry. After statistical testing using ANOVA, 115 proteins were found to be significantly changed in h- α S overexpressing mouse brains compared to controls. Considering only hits with at least two unique peptides identified left 42 differentially expressed proteins (see Supplementary Table S2, online resource). Furthermore, the overexpression of human α -syn in the h- α S mice on the protein level was confirmed by Western blots of homogenates and S-synaptosomes (Supplementary Fig. 1a,

online resource) and quantitative MS data of FASS synaptosomes (Supplementary Fig. 1b, online resource).

Overexpression of α -syn induces an increased expression of proteins at synapses

Of the 42 differentially expressed proteins, the majority displayed an increased abundance in h- α S samples (Fig. 2a). Therefore, we tested whether this trend may result from structural alterations, e.g., an increased number of synaptic vesicles per presynapse. We therefore performed transmission electron microscopy and measured the presynaptic area, the postsynaptic density length, the number and density of synaptic vesicles. We did not observe any difference between control and h- α S mice on any of these parameters (Supplementary Fig. 2, online resource).

Among the significantly upregulated targets are proteins of the endocytic machinery (Ap2a1, Ap2b1), intracellular trafficking-related Rab GTPases (Rab1b, Rab3a), regulators of ER structure and function (Rtn4, Rtn1) and Ca²⁺ homeostasis (Ppp3r1), cytoskeleton and associated proteins

[Tuba4a, Tubb2a/3/4a/5, Actn1, Mapt (also known as tau)], mitochondrial proteins (Ndufv1, Ndufs6), synaptic vesicle proteins (Syngn1, Syngn3) and the synaptic vesicle exocytosis regulator Stxbp1, also known as Munc-18-1. The 42 proteins that we found to be significantly enriched or depleted in our PDGF-h- α S \times VGLUT1^{VENUS} samples were further classified according to their ascribed cellular localization and molecular function using gene ontology (GO) terms (Supplementary Fig. 3a, online resource).

To validate the proteomic analysis, we performed a series of Western blots on homogenates and conventional S-synaptosomes (Supplementary Fig. 3b, Supplementary Fig. 4, online resource) as well as quantitative immunofluorescence imaging on VGLUT1^{VENUS} FASS synaptosomes targeting several protein hits. While no h- α S-related changes could be detected in homogenates, we observed a significant increase of synaptogyrin 1 and Munc18-1 in S-synaptosomes. Increased levels of β -tubulin, synaptogyrin 3, and tau were not yet confirmed (Supplementary Fig. 3c–e, online resource).

Besides the overexpressed proteins, two proteins were found to be significantly reduced in abundance, the small proline-rich protein 2B (Sprr2B) and the eukaryotic translation elongation factor 1 alpha 1 (eEF1A1), which were reduced down to about 13% and 8%, respectively, of their mean normalized abundances in controls (Supplementary Table S2, online resource). While the synaptic functions of Sprr2B are unknown, eEF1A1 has, apart from its role as a translation factor, several non-canonical functions in synaptic plasticity and was therefore regarded with special attention in the present study.

Bioinformatic cluster analysis indicates α -syn-mediated disruption of the synaptic protein network

To better understand which cellular pathways are altered in response to α -syn overexpression, we performed KEGG pathway and gene ontology (GO) term analyses on the proteins which were found to be differentially expressed in h- α S mice (Fig. 2b).

KEGG pathway enrichment analysis showed those pathways significantly enriched which contribute to neurotransmitter release, such as ‘synaptic vesicle cycle’ or ‘calcium reabsorption’. Furthermore, pathways related to Alzheimer’s disease and Huntington’s disease were significantly enriched (Fig. 2b). Similarly, GO classification revealed molecular functions related to neurotransmission, such as ‘GTPase activity’ and ‘GTP binding’, which are involved in vesicle cycling via small G-proteins and presynaptic modulation of transmitter release via G-protein coupled neurotransmitter receptors (Supplementary Fig. 3a, online resource).

To determine the network of proteins interacting with those that were differentially expressed in tissue overexpressing α -syn, we performed an IntAct database analysis using DAVID Bioinformatics Resources 6.8 [42, 43]. This revealed, among others, a number of 14-3-3 constituents (Ywhab, Ywhaz and Ywhae), which are known for their interaction with α -syn aggregation intermediates and their presence in Lewy bodies [63]. Additional interaction partners were, for example, PSD95 (Dlg4) or NMDA channel subunits (Grin2b, Grin1) (Fig. 2c). While these were, as expected by the input, proteins typically involved in synaptic function, eEF1A1 was listed as an interaction partner in a majority of the results (Supplementary Table S3, online resource). These results suggest that eEF1A1 may play a critical role in the regulation of synaptic function. We therefore decided to further characterize eEF1A1 in h- α S mice and human cases of Lewy body disease.

Validation of the differential expression of eEF1A1 in synaptosomes

Quantitative MS data showed a marked reduction in the normalized abundance of eEF1A1 in PDGF-h- α S \times VGLUT1^{VENUS} FASS synaptosomes, with a fold change of 0.08 compared to control. To confirm this downregulation, Western blots were performed with the homogenates and S-synaptosomal fractions. While the eEF1A1 level was significantly lower in S-synaptosomes of h- α S animals compared to wild-type littermates, it was unchanged in homogenates (Fig. 3a).

During FASS, 10⁶ FASS synaptosomes per sample were further collected and fixed on glass coverslips. Immunofluorescence confocal imaging followed by analysis of VGLUT1^{VENUS} and eEF1A1 intensities allowed to confirm the local reduction of eEF1A1 signal at individual VGLUT1^{VENUS} FASS synaptosomes (Fig. 3b). Figure 3c shows eEF1A1 immunosignal projections from 48 randomly selected FASS synaptosomes, aligned for better representation. In the sample from α S overexpressing animals (Fig. 3c2), the signal is reduced, which is especially relevant for structures expressing larger amounts of eEF1A1. The cumulative frequency distribution of the relative eEF1A1/VGLUT1^{VENUS} fluorescence shows a shift to the left in α S samples compared to controls, confirming lower eEF1A1 signal in these synaptosomes (Fig. 3d). A reduction of the integrated eEF1A1 immunofluorescence in relation to VGLUT1^{VENUS} signal intensity can also be observed in a representation of all imaged FASS synaptosomes ($n = 630$ – 755 measurements per sample) (Fig. 3e). Consequently, the mean relative eEF1A1 intensity is significantly lower in FASS VGLUT1^{VENUS} synaptosomes derived from α S animals (Fig. 3f).

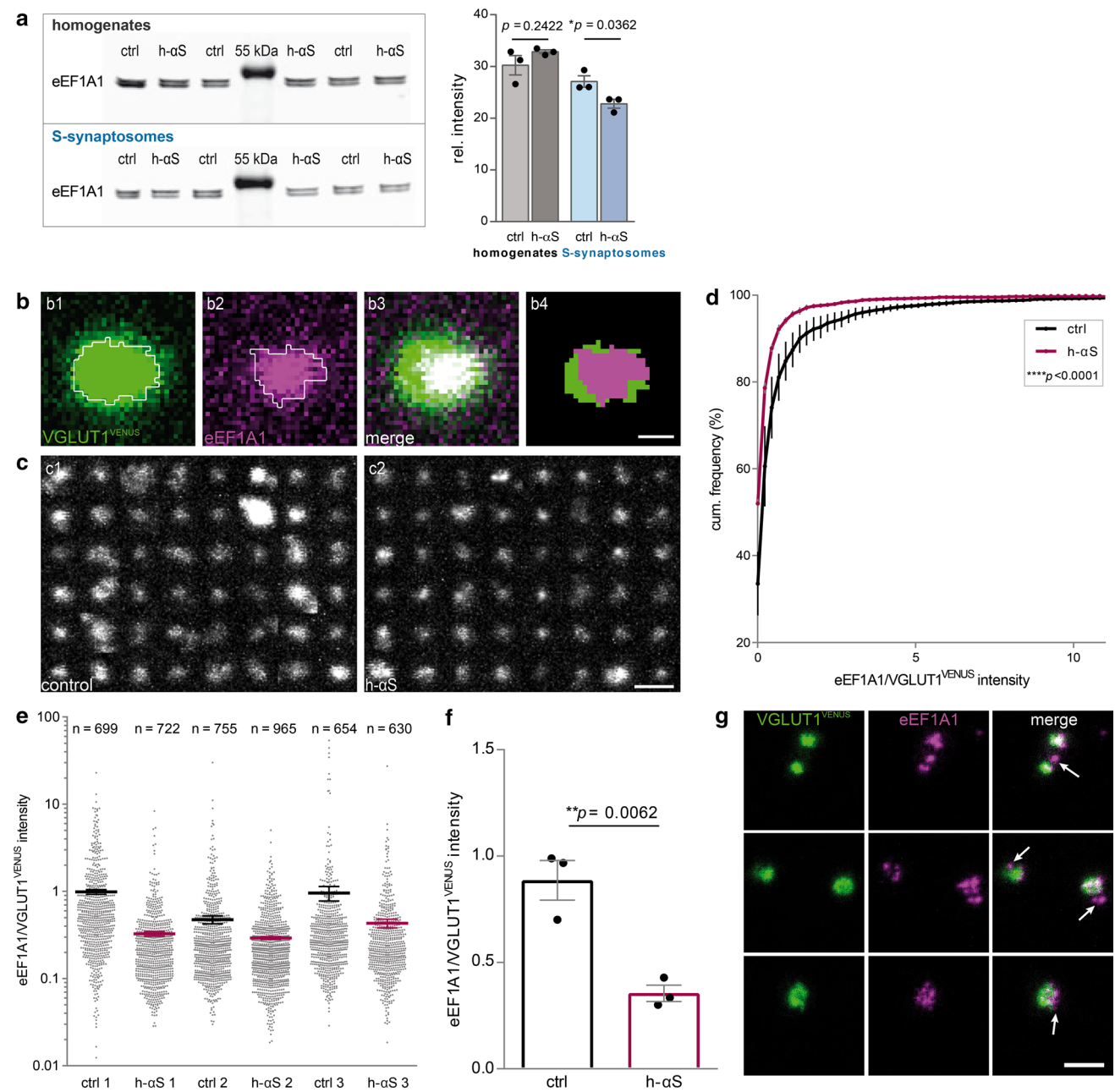


Fig. 3 eEF1A1 is reduced in synaptosomes of h- α S mice. **a** Western blot of homogenates and S-synaptosomes. $n = 3$ mice per group, mean with s.e.m., Student's t test; $*p < 0.05$. **b** Example quantification of individual FASS synaptosomes. b1 VGLUT1^{VENUS} fluorescence (green) was used to detect the volume of a synaptosome (delineated with white line). b2 Immunofluorescence of the second marker (here eEF1A1 in magenta) was used to detect volume of associated marker (delineated with white line). b3 Overlay of VGLUT1^{VENUS} and eEF1A1 immunofluorescence. b4 Overlay of the detected synaptosome and the associated eEF1A1-positive structure. Scale bar = 1 μ m. **c** 48 randomly selected eEF1A1-positive synapses displayed as

a gallery for control (c1) and h- α S (c2) mice; scale bar = 2 μ m. **d** Cumulative frequency of eEF1A1/VGLUT1^{VENUS} fluorescence signals; Kolmogorov–Smirnov test; **** $p < 0.0001$. **e** Intensity signals from all FASS synaptosomes quantified, as eEF1A1/VGLUT1^{VENUS} ratios. **f** Mean eEF1A1/VGLUT1^{VENUS} signals. $n = 3$ mice per group, mean with s.e.m., Student's t test; ** $p < 0.01$. **g** STED microscopy of eEF1A1 and VGLUT1^{VENUS} signals reveals the location of eEF1A1 at both pre- and postsynapses: arrows point to eEF1A1-positive structures excluded from the VGLUT1^{VENUS} positive presynapse, likely belonging to the postsynaptic compartment; scale bar = 1 μ m

As synaptosomes consist mainly of the resealed presynaptic element associated to the unsealed tip of the postsynaptic spine [7, 37], we further determined eEF1A1 protein

subcellular localization using STED microscopy with a resolution of 60 nm. In most synaptosomes, eEF1A1 immunofluorescence colocalized with VGLUT1^{VENUS} signal, while

additional dots were opposed to presynapses (Fig. 3g). We therefore conclude that the eEF1A1 protein is present on both sides of synapses and may be directly impacted by presynaptic pathological processes induced by α -syn.

eEF1A1 is reduced in the brain tissue of h- α S mice

As we were interested in the expression and distribution of eEF1A1 in intact tissue, we next examined eEF1A1 protein levels in brain tissue of 12-week-old PDGF-h- α S \times VGLUT1^{VENUS} mice. Two brain regions were investigated using immunofluorescence staining against eEF1A1 and confocal microscopy: layer I of the cingulate cortex and the somatosensory cortex (Fig. 4a), in which data on spine loss had been acquired previously. The fluorescence intensity of eEF1A1-positive puncta as well as their number was analyzed (Fig. 4b). We found a strong reduction in eEF1A1 staining intensity in both the cingulate and the somatosensory cortex (Fig. 4c, Supplementary Fig. 5a, online resource). As in one of the brain areas a small but significant difference in endogenous VGLUT1^{VENUS} expression was measured (Supplementary Fig. 5b, online resource), we used the mean eEF1A1/VGLUT1^{VENUS} fluorescence intensity for statistical comparison. The ratio proved to be profoundly reduced in h- α S tissue (Fig. 4d). Additionally, a reduction of the density of eEF1A1-positive puncta was detected in the two cortical areas of h- α S mice (Fig. 4e), whereas the mean puncta volume was unchanged between groups (Supplementary Fig. 5c, online resource).

Similarly, we approached the question whether a change in the amount of excitatory postsynapses is present in this mouse brain tissue. Correlating with the loss of eEF1A1 in h- α S mouse samples, we indeed observed reduced PSD95 immunofluorescence intensity in these brains (Fig. 4f, g), accompanied by a loss of PSD95-positive structures in the tissue (Fig. 4h). In this way, we confirm that spine loss is present at 12 weeks in h- α S mice and at the time of experimental procedures in this study.

eEF1A1 is reduced in the neuropil of human LBD cases

To translate our findings to human cases, we investigated the expression of eEF1A1 in the cingulate gyrus of LBD brains compared to age-matched controls. In homogenates from the cingulate cortex, we did not observe a significant difference in eEF1A1 levels between control and LBD brains (Fig. 5a, b). Noticeably, PSD95 expression was reduced in LBD brains (Fig. 5a, c), indicating a loss of cortical synapses. We therefore applied IHC to assess potential changes of eEF1A1 expression in the neuropil. We included tissue from mid-stage (Braak stages 3 or 4) and late-stage (Braak stages 5 or 6) LBD patients. Late-stage LBD cases featured

significant α -syn pathology in the cingulate cortex (Fig. 5d and Supplementary Fig. 6a, online resource), whereas in mid-stage LBD, no α -syn pathology can be detected in the cingulate cortex. We performed eEF1A1 IHC on formalin-fixed, paraffin-embedded tissue sections from the human cingulate gyrus. LBD cases from both mid- and late-stage groups showed less intense DAB staining patterns compared to controls (Fig. 5e, Supplementary Fig. 6b, online resource). Strikingly, quantification of the DAB signal for eEF1A1 revealed significantly reduced values in the cortical layer I neuropil of LBD brains, whereas the DAB staining intensity within cell bodies was comparable between groups (Fig. 5f, Supplementary Fig. 6c, online resource). Existing co-pathologies or variation in post-mortem delay (PMD) had no effect on this observation (Supplementary Fig. 7, online resource). This indicates that α -syn-mediated reduction in eEF1A1 is not only present in the tissue of our mouse model, but also in human cases of LBD and that in both cases, this reduction is mainly at the level of synapses.

Discussion

Synapses are vulnerable to misfolded protein species like α -syn and their degeneration is crucially involved in the pathogenesis of neurodegenerative diseases [12]. Moreover, dendritic spine loss has been described as a structural correlate for cognitive impairment and dementia [4, 25, 62, 73]. We show that spine loss is present in h- α S mice at the age of 18 weeks compared to both 8-week-old h- α S mice and age-matched controls. In a previous *in vivo* imaging study, we observed progressive spine loss in the cerebral cortex of mice overexpressing α -syn between 12 and 17 weeks of age [8], which precedes the onset of motor impairments by several months [2, 52]. Based on this knowledge, we aimed to elucidate changes on the protein level in excitatory synapses that might explain the early synaptopathy induced by α -syn overexpression. We used FASS of VGLUT1^{VENUS} expressing synapses to achieve a two to threefold enrichment of glutamatergic synaptosomes compared to conventional preparations. Using highly sensitive proteomic analyses on FASS samples, we detected more than 600 synaptic proteins, out of which 42 were differentially expressed in samples overexpressing human α -syn. Among those, only two proteins were reduced, while the others show an increase in protein levels.

Although FASS provides limited amounts of synaptosome material for analysis, the removal of extra-synaptic compartments allowed us to obtain valuable and valid results with regards to existing literature on α -syn function and pathogenicity at glutamatergic synapses. The facts that the average level of VGLUT1 is unaffected in our samples prior to sorting and that the differential expression of identified

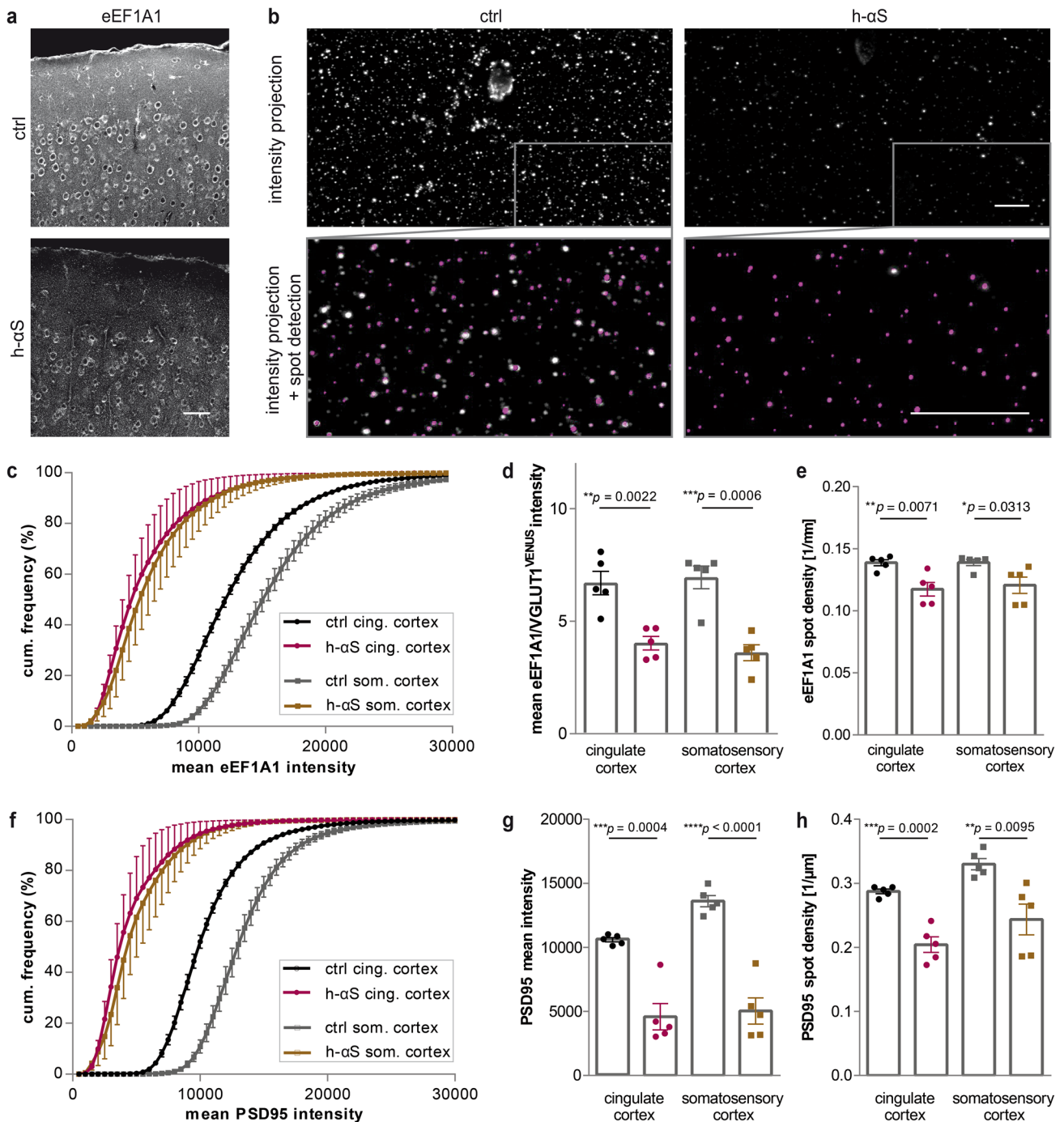


Fig. 4 eEF1A1 is reduced in the h- α S mouse cortex and is correlated with a reduction in PSD95. **a** Representative images of mouse somatosensory cortex stained for eEF1A1; scale bar = 50 μ m. **b** Top: maximum intensity projections of cortical layer I field of view. Bottom: magnified area from top panel illustrating spot detection (magenta). Scale bars = 10 μ m. **c** Cumulative distribution of the mean eEF1A1 intensity. The curves of h- α S mice show a strong left shift towards

less intense values. **d** Mean eEF1A1/VGLUT1^{VENUS} ratio of fluorescence intensity. **e** Reduced density/ μ m of eEF1A1-positive spots in h- α S mice. **f** Cumulative distribution of the mean PSD95 intensity. **g** Mean PSD95 fluorescence intensity is reduced in h- α S mice. **h** Reduction of PSD95 spot density/ μ m in h- α S mice. $n=5$ mice per group, mean with s.e.m., Student's t test; * $p < 0.05$, ** $p < 0.01$, *** $p < 0.001$, **** $p < 0.0001$

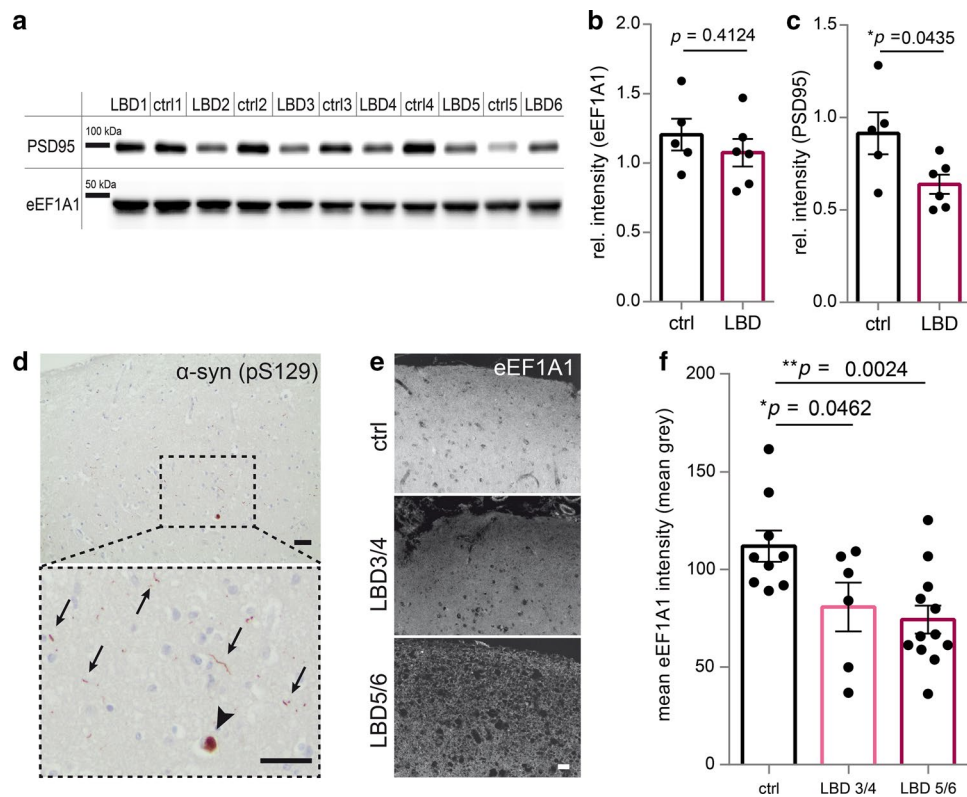


Fig. 5 eEF1A1 expression is reduced in post-mortem human neuropil of LBD patients. **a** Western blot of cingulate cortex homogenate. **b, c** eEF1A1 levels are similar in homogenates of human cingulate cortex, PSD95 expression is reduced in advanced LBD (Braak 5/6). $n=5$ (control) and $n=6$ (LBD), mean with s.e.m., Student's *t* test; $*p < 0.05$. **d** Deposits of phospho- α -syn are present as Lewy bodies (arrowhead) and Lewy neurites (arrows) in the cingulate gyrus

of late-stage LBD. Image from the same brain as in **e** (LBD 5/6). **e** Exemplary eEF1A1 staining in human cingulate gyrus from a control, mid-stage (Braak 3/4) and late-stage (Braak 5/6) LBD case, respectively. **f** eEF1A1 staining intensity is reduced in layer I of the cingulate gyrus of LBD brains. $n=9$ (ctrl), $n=6$ (LBD 3/4), $n=12$ (LBD 5/6), mean with s.e.m., Student's *t* test; $*p < 0.05$, $**p < 0.01$. Scale bars = 20 μ m

proteins was not detected on our homogenates and—in most cases—S-synaptosomes indicate that local defects at glutamatergic synapses rather than global defects at the neuron level are present at the onset of disease progression. Our experiments suggest α -syn-related changes in vesicle trafficking, cytoskeleton, ER- and Ca^{2+} homeostasis and mitochondrial metabolism.

Synucleins are known to be involved in the trafficking of synaptic vesicles [24, 31, 48, 59, 67, 81]. We identified upregulation of several proteins important for the synaptic vesicle cycle (Syngr1, Syngr3, Rab3A, Munc18-1, Nsf, Ap2a1, Ap2b1, Ap2m1, Sh3glb2). Previous studies in LBD and α -syn mouse models have shown an abnormal interaction between α -syn and Rab3A, Rab5 and Rab8, thereby disrupting endocytic and secretory pathways [75, 78]. In our proteomic screen, we also found the synaptic vesicle proteins Syngr1 and Munc18-1 elevated in h- α S mice, which was confirmed by Western blot of S-synaptosomes, but not of homogenates. Apart from its role in regulation of exocytosis, Munc18-1 has been shown to serve as a chaperone controlling α -syn aggregation [16] and its upregulation

might counteract both directly the aggregation propensity of α -syn by stabilizing the aggregation-resistant membrane-bound forms of α -syn and indirectly a decrease in functional Munc18-1 for secretion of synaptic vesicles due to co-aggregation with α -syn.

Similarly, α -syn directly interacts with members of the cytoskeleton like β III-tubulin and the microtubule-associated protein tau (Mapt) [15]. Native α -syn also acts as a microtubule-associated protein, facilitating microtubule polymerization and neurite outgrowth in cultured neurons [47]. In the pathologic condition, its interaction with tubulin and tau facilitates intracellular α -syn accumulation, impairing microtubule stability and microtubule-mediated transport [58, 64, 71]. A recent study reveals synaptogyrin-3 as specific interactor of mislocalized, presynaptic tau, restricting synaptic vesicle mobility and driving defects in neurotransmission in fly and mouse models of tauopathy [55]. Both Syngr3 and tau were found to be elevated in our proteomic data from h- α S mice, along with several tubulin subunits (Tuba4a, Tubb2a/3/4a/5). Though validation analysis revealed a trend towards an increase

for Syngn3 and Tau in S-synaptosomes and for Syngn3, tau and β -tubulin in FASS synaptosomes without reaching significance, further investigations will be required to confirm the upregulation of those targets. Our results provide evidence for disease-related alterations of cytoskeletal and synaptic vesicle dynamics and open perspectives for future research.

A further line of evidence in our proteomic study implies the involvement of organelles and proteins regulating cytosolic Ca^{2+} homeostasis, which are found elevated in our h- α S FASS synaptosomes (Ppp3r1, Rtn4, Rtn1, Ndufs6, Ndufv1). Indeed, previous work identified that increasing levels of α -syn proportionally increase cytoplasmic Ca^{2+} concentrations and drive cascade engaging calcineurin (Ppp3r1) and substrates that result in toxicity in mammalian cells [13]. Similarly, the reticulon proteins (Rtn4, Rtn1) are regulators of ER structure and Ca^{2+} homeostasis and have a proapoptotic function mediated by the induction of ER stress [23]. Several proteins of our screen further point towards alterations in mitochondrial energy metabolism, which is in line with previous studies on Parkinson's disease [41]. Wild-type α -syn is present in mitochondria-associated ER membranes (MAM), regulating the mitochondrial calcium homeostasis [11, 36]. Finally, α -syn has also been shown to directly induce changes in mitochondria fission [57].

The translation factor eEF1A1 stands out by its strong depletion in our h- α S FASS synaptosomes. We validated our finding in S-synaptosomes as well as in FASS synaptosomes originating from the same mice as the proteomic data. The translation capacity of eEF1A1 and its potential to regulate actin dynamics and spine size predestine it for the control of synaptic plasticity at the protein level. Together with other proteins locally translated at synapses, a functional synergy to maintain long-term potentiation (LTP) by signaling through the mTOR pathway is established [74]. Additionally, the expression of eEF1A1 at nerve terminals has been shown to be essential for maintaining newly grown synapses [33].

Both pre- and postsynaptic compartments have previously been demonstrated to express eEF1A1, which is in line with our observations. Using STED microscopy, we found the eEF1A1 immunosignal both colocalized with and excluded from VGLUT1^{VENUS} fluorescence in single excitatory synaptosomes. On the presynaptic side, eEF1A1 transcripts are enriched in mature CNS axons and are reduced following axonal injury [72]. An increasing literature support the notion that the protein synthesis machinery is active within CNS axons and involved in synaptic plasticity [69]. Furthermore, several translation factor mRNAs including eEF1a1 mRNA have been reported at the local transcriptome of presynapses [37], it is therefore likely that eEF1A1 expression can be differentially regulated between the soma and synapses. FASS provides a powerful tool to detect such local

changes, which may be masked by the proportionately large abundance in somata in less enriched preparations.

eEFs also link up with the p70S6K pathway to protein expression in neurites and synapses, where they promote NGF-induced neurite outgrowth [38, 44, 61], synapse formation and stabilization. Likewise, eEF1A1 has been convincingly shown to be associated with dendrites and excitatory postsynapses and more specifically, the postsynaptic density within dendritic spines via binding actin [17, 18, 28]. Moreover, eEF1A1 knockdown significantly decreases PSD95 expression levels in vitro [30]. Here, we extend this knowledge to the mouse brain, showing that a reduction of eEF1A1 is concomitant with a reduction in PSD95 intensity and spot density at the observed age. It connects our previous finding of commencing dendritic spine loss [8] to other, non-canonical functions of eEF1A1. eEF1A1 regulates cytoskeletal dynamics by bundling F-actin and binding to microtubules [10, 35, 46, 82], acts protective against apoptosis [65] and regulates M4 muscarinic acetylcholine receptor recycling [54] and protein degradation [19]. Furthermore, a recent study demonstrated that a CTIF–eEF1A1–DCTN complex links selective recognition and aggresomal targeting of misfolded α -syn. This process is accompanied by a sequestration of CTIF and possibly eEF1A1 into the aggresome, which might in turn decrease the amount of synaptic eEF1A1 [60]. Additionally, α -syn toxicity and the corresponding elevation of synaptic Ca^{2+} could disrupt eEF1A1 dimer formation and lead to decreased F-actin bundling impairing spine stabilization [10].

Strikingly, human brain tissue from LBD patients also showed reduced eEF1A1 staining intensity in the densely synaptic layer I of the cingulate cortex. We observed this in advanced stages of the disease (Braak 5/6) but also in earlier stages (Braak 3/4) in which no visible α -syn pathology is present in the cingulate cortex and the neocortex. At the same time, differences in eEF1A1 expression were not detectable in cortex homogenates of late-stage LBD, whereas a reduction of overall PSD95 expression was present. Together, these results indicate a local pathophysiological role for eEF1A1 at synapses early in the disease progression. As de novo protein synthesis and cytoskeleton remodeling links chemically or electrically induced changes in synaptic strength to structural adaptations, it is the basis for memory consolidation in the brain and depletion of eEF1A1 can contribute to structural impairments observed in neurodegenerative conditions. In fact, a study in Alzheimer's disease brains has connected dysregulated eEF1A expression to synaptic plasticity impairments [3] and defects in de novo protein synthesis have been demonstrated in several neurodegenerative disorders characterized by impaired synaptic plasticity, including Parkinson's disease, Alzheimer's disease, frontotemporal lobar degeneration and prion diseases [22, 32, 51, 56]. eEF1A1 may therefore serve as a

universal marker for neurodegenerative diseases characterized by synapse loss, yet future research is needed for tying together these lines of evidence.

Our study highlights for the first time the functional role of eEF1A1 in α -synucleinopathies and opens new perspectives about the involvement of eEF1A1 in α -synucleinopathies. We therefore propose a model, in which synaptic eEF1A1 reduction is an early and central event, which is caused by a disruption of α -syn balance and may mediate alterations in the organization of the cytoskeleton, phagosomal activity and ultimately leads to synaptopathy. By altering the normal half-life of eEF1A1, estimated to be 4.7 days [20], α -syn overexpression might furthermore indirectly affect the turnover of other presynaptic proteins and approaching this question could be subject to future research. A more detailed understanding of the role of eEF1A proteins in the pathogenesis of α -synucleinopathies still remains to be determined. It will be important to investigate the mechanistic link between synaptic translation and α -syn-mediated synaptopathy in the future and to determine whether eEF1A1 or its upstream factors like the eukaryotic initiation factor 2 α (eIF2 α) represent genuine targets for novel therapeutic approaches.

Acknowledgements We thank Sarah Hanselka, Katharina Bayer, Michael Schmidt, Dr. Christelle Martin, Melissa Deshors, Dr. Norbert Buresch (Neurobiobank Munich), Dr. Vincent Pitard (Flow cytometry facility, CNRS UMS 3427, INSERM US 005, Univ. Bordeaux), Patrice Mascalchi (Bordeaux Imaging Center, CNRS, INSERM, Univ. Bordeaux) and the Biochemistry and biophysics facility of Bordeaux Neurocampus (CNRS, INSERM, Univ. Bordeaux) for their excellent technical support and animal care. We are also thankful towards Stephan Müller for his expertise in proteomics and advice on our data.

Author contributions SB performed design of the experiment, subcellular fractionation, FASS sorting, validation of results in mouse and human tissue, bioinformatics and interpretation of results and wrote the manuscript. MFA provided expertise and performed subcellular fractionation, FASS sorting and Western blotting with SB. FP performed programming for image analysis. MMD performed bioinformatic analyses. MMD, VCR and TA selected human tissue and provided neuropathological expertise. ML performed EM experiments and EM data analysis. SCI performed mass spectrometry and analysis of the MS raw data. EH performed STED microscopy. SCr and LS provided technical support. VCR, MMD, MFA, EH and JH helped with manuscript preparation. EH and JH supervised the study, contributed to conception, design and manuscript writing and provided financial support and final approval of the manuscript.

Funding This work was funded by the Munich Cluster for Systems Neurology SyNergy (EXC1010) to SB, SC and JH; the German Academic Exchange Service (DAAD) to SB; the French Agence Nationale de la Recherche (ANR-12-JSV4-0005-01VGLUT-IQ and ANR-10-LABX-43 BRAIN) to EH; the Fondation pour la Recherche Médicale (ING20150532192) to EH and the CNRS PICS program to EH.

Compliance with ethical standards

Conflict of interest The authors declare that they have no conflict of interest.

Ethical approval All procedures performed in studies involving human participants were in accordance with the ethical standards of the institutional and/or national research committee and with the 1964 Helsinki Declaration and its later amendments or comparable ethical standards. All applicable international, national, and/or institutional guidelines for the care and use of animals were followed.

References

1. Abbas W, Kumar A, Herbein G (2015) The eEF1A proteins: at the crossroads of oncogenesis, apoptosis, and viral infections. *Front Oncol* 5:75. <https://doi.org/10.3389/fonc.2015.00075>
2. Amschl D, Neddens J, Havas D, Flunkert S, Rabl R, Römer H, Rockenstein E, Masliah E, Windisch M, Hutter-Paier B (2013) Time course and progression of wild type α -Synuclein accumulation in a transgenic mouse model. *BMC Neurosci* 14:1
3. Beckelman BC, Day S, Zhou X, Donohue M, Gouras GK, Klann E, Keene CD, Ma T (2016) Dysregulation of elongation factor 1A expression is correlated with synaptic plasticity impairments in Alzheimer's disease. *J Alzheimers Dis JAD* 54:669–678. <https://doi.org/10.3233/JAD-160036>
4. Bellucci A, Zaltieri M, Navarra L, Grigoletto J, Missale C, Spano P (2012) From α -synuclein to synaptic dysfunctions: new insights into the pathophysiology of Parkinson's disease. *Brain Res* 1476:183–202. <https://doi.org/10.1016/j.brainres.2012.04.014>
5. Ben Gedalya T, Loeb V, Israeli E, Altschuler Y, Selkoe DJ, Sharon R (2009) α -Synuclein and polyunsaturated fatty acids promote clathrin-mediated endocytosis and synaptic vesicle recycling. *Traffic* 10:218–234. <https://doi.org/10.1111/j.1600-0854.2008.00853.x>
6. Bendor JT, Logan TP, Edwards RH (2013) The function of α -synuclein. *Neuron* 79:1044–1066. <https://doi.org/10.1016/j.neuron.2013.09.004>
7. Biesemann C, Grønberg M, Luquet E, Wichert SP, Bernard V, Bungers SR, Cooper B, Varoqueaux F, Li L, Byrne JA, Urlaub H, Jahn O, Brose N, Herzog E (2014) Proteomic screening of glutamatergic mouse brain synaptosomes isolated by fluorescence activated sorting. *EMBO J* 33:157–170. <https://doi.org/10.1002/embj.201386120>
8. Blumenstock S, Rodrigues EF, Peters F, Blazquez-Llorca L, Schmidt F, Giese A, Herms J (2017) Seeding and transgenic overexpression of alpha-synuclein triggers dendritic spine pathology in the neocortex. *EMBO Mol Med* 9:716–731. <https://doi.org/10.15252/emmm.201607305>
9. Braak H, Del Tredici K, Rüb U, de Vos RA, Steur ENJ, Braak E (2003) Staging of brain pathology related to sporadic Parkinson's disease. *Neurobiol Aging* 24:197–211
10. Bunai F, Ando K, Ueno H, Numata O (2006) Tetrahymena eukaryotic translation elongation factor 1A (eEF1A) bundles filamentous actin through dimer formation. *J Biochem (Tokyo)* 140:393–399. <https://doi.org/10.1093/jb/mvj169>
11. Cali T, Ottolini D, Negro A, Brini M (2012) α -Synuclein controls mitochondrial calcium homeostasis by enhancing endoplasmic reticulum–mitochondria interactions. *J Biol Chem* 287:17914–17929. <https://doi.org/10.1074/jbc.M111.302794>

12. Calo L, Wegrzynowicz M, Santivañez-Perez J, Grazia Spillantini M (2016) Synaptic failure and α -synuclein. *Mov Disord* 31:169–177. <https://doi.org/10.1002/mds.26479>
13. Caraveo G, Auluck PK, Whitesell L, Chung CY, Baru V, Mosharov EV, Yan X, Ben-Johny M, Soste M, Picotti P, Kim H, Caldwell KA, Caldwell GA, Sulzer D, Yue DT, Lindquist S (2014) Calcineurin determines toxic versus beneficial responses to -synuclein. *Proc Natl Acad Sci* 111:E3544–E3552. <https://doi.org/10.1073/pnas.1413201111>
14. Carpenter AE, Jones TR, Lamprecht MR, Clarke C, Kang IH, Friman O, Guertin DA, Chang JH, Lindquist RA, Moffat J, Golland P, Sabatini DM (2006) Cell Profiler: image analysis software for identifying and quantifying cell phenotypes. *Genome Biol* 7:R100. <https://doi.org/10.1186/gb-2006-7-10-r100>
15. Cartelli D, Aliverti A, Barbiroli A, Santambrogio C, Ragg EM, Casagrande FVM, Cantele F, Beltramone S, Marangon J, De Gregorio C, Pandini V, Emanuele M, Chieriegatti E, Pieraccini S, Holmqvist S, Bubacco L, Roybon L, Pezzoli G, Grandori R, Arnal I, Cappelletti G (2016) α -Synuclein is a novel microtubule dynamase. *Sci Rep* 6:33289. <https://doi.org/10.1038/srep33289>
16. Chai YJ, Sieracki E, Tomatis VM, Gormal RS, Giles N, Morrow IC, Xia D, Götz J, Parton RG, Collins BM, Gambin Y, Meunier FA (2016) Munc18-1 is a molecular chaperone for α -synuclein, controlling its self-replicating aggregation. *J Cell Biol* 214:705–718. <https://doi.org/10.1083/jcb.201512016>
17. Cho S-J, Jung J-S, Ko BH, Jin I, Moon IS (2004) Presence of translation elongation factor-1A (eEF1A) in the excitatory postsynaptic density of rat cerebral cortex. *Neurosci Lett* 366:29–33. <https://doi.org/10.1016/j.neulet.2004.05.036>
18. Cho S-J, Lee H-S, Dutta S, Seog D-H, Moon I-S (2012) Translation elongation factor-1A1 (eEF1A1) localizes to the spine by domain III. *BMB Rep* 45:227–232. <https://doi.org/10.5483/BMBRep>
19. Chuang S-M, Chen L, Lambertson D, Anand M, Kinzy TG, Madura K (2005) Proteasome-mediated degradation of cotranslationally damaged proteins involves translation elongation factor 1A. *Mol Cell Biol* 25:403–413. <https://doi.org/10.1128/MCB.25.1.403-413.2005>
20. Cohen LD, Zuchman R, Sorokina O, Müller A, Dieterich DC, Armstrong JD, Ziv T, Ziv NE (2013) Metabolic turnover of synaptic proteins: kinetics, interdependencies and implications for synaptic maintenance. *PLoS ONE* 8:e63191. <https://doi.org/10.1371/journal.pone.0063191>
21. De Robertis E, De Lores Rodriguez, Arnaiz G, Pellegrino De Iraldi A (1962) Isolation of synaptic vesicles from nerve endings of the rat brain. *Nature* 194:794–795
22. Delaidelli A, Jan A, Herms J, Sorensen PH (2019) Translational control in brain pathologies: biological significance and therapeutic opportunities. *Acta Neuropathol (Berl)* 137:535–555. <https://doi.org/10.1007/s00401-019-01971-8>
23. Di Sano F, Piacentini M (2012) Reticulon protein-1C: a new hope in the treatment of different neuronal diseases. *Int J Cell Biol* 2012:1–9. <https://doi.org/10.1155/2012/651805>
24. Diao J, Burré J, Vivona S, Cipriano DJ, Sharma M, Kyoung M, Südhof TC, Brunger AT (2013) Native α -synuclein induces clustering of synaptic-vesicle mimics via binding to phospholipids and synaptobrevin-2/VAMP2. *eLife*. <https://doi.org/10.7554/eLife.00592>
25. Dickson DW, Crystal HA, Bevona C, Honer W, Vincent I, Davies P (1995) Correlations of synaptic and pathological markers with cognition of the elderly. *Neurobiol Aging* 16:285–298. [https://doi.org/10.1016/0197-4580\(95\)00013-5](https://doi.org/10.1016/0197-4580(95)00013-5)
26. Dieterich DC, Kreutz MR (2016) Proteomics of the synapse—a quantitative approach to neuronal plasticity. *Mol Cell Proteom* 15:368–381. <https://doi.org/10.1074/mcp.R115.051482>
27. Emanuele M, Esposito A, Camerini S, Antonucci F, Ferrara S, Seghezza S, Catelani T, Crescenzi M, Marotta R, Canale C, Matteoli M, Menna E, Chieriegatti E (2016) Exogenous alpha-synuclein alters pre- and post-synaptic activity by fragmenting lipid rafts. *EBioMedicine* 7:191–204. <https://doi.org/10.1016/j.ebiom.2016.03.038>
28. Fernández E, Collins MO, Uren RT, Kopanitsa MV, Komiyama NH, Croning MDR, Zografos L, Armstrong JD, Choudhary JS, Grant SGN (2009) Targeted tandem affinity purification of PSD-95 recovers core postsynaptic complexes and schizophrenia susceptibility proteins. *Mol Syst Biol* 5:269. <https://doi.org/10.1038/msb.2009.27>
29. Fortin DL (2004) Lipid rafts mediate the synaptic localization of α -synuclein. *J Neurosci* 24:6715–6723. <https://doi.org/10.1523/JNEUROSCI.1594-04.2004>
30. Fujimura M, Usuki F, Cheng J, Zhao W (2016) Prenatal low-dose methylmercury exposure impairs neurite outgrowth and synaptic protein expression and suppresses TrkA pathway activity and eEF1A1 expression in the rat cerebellum. *Toxicol Appl Pharmacol* 298:1–8. <https://doi.org/10.1016/j.taap.2016.03.002>
31. Fusco G, Pape T, Stephens AD, Mahou P, Costa AR, Kaminski CF, Kaminski Schierle GS, Vendruscolo M, Veglia G, Dobson CM, De Simone A (2016) Structural basis of synaptic vesicle assembly promoted by α -synuclein. *Nat Commun* 7:12563. <https://doi.org/10.1038/ncomms12563>
32. García-Esparcia P, Hernández-Ortega K, Koneti A, Gil L, Delgado-Morales R, Castaño E, Carmona M, Ferrer I (2015) Altered machinery of protein synthesis is region- and stage-dependent and is associated with α -synuclein oligomers in Parkinson's disease. *Acta Neuropathol Commun* 3:76. <https://doi.org/10.1186/s40478-015-0257-4>
33. Giustetto M, Hegde AN, Si K, Casadio A, Inokuchi K, Pei W, Kandel ER, Schwartz JH (2003) Axonal transport of eukaryotic translation elongation factor 1 α mRNA couples transcription in the nucleus to long-term facilitation at the synapse. *Proc Natl Acad Sci* 100:13680–13685
34. Gray EG, Whittaker VP (1962) The isolation of nerve endings from brain: an electron-microscopic study of cell fragments derived by homogenization and centrifugation. *J Anat* 96:79–88
35. Gross SR, Kinzy TG (2005) Translation elongation factor 1A is essential for regulation of the actin cytoskeleton and cell morphology. *Nat Struct Mol Biol* 12:772–778. <https://doi.org/10.1038/nsmb979>
36. Guardia-Laguarta C, Area-Gomez E, Rub C, Liu Y, Magrane J, Becker D, Voos W, Schon EA, Przedborski S (2014) α -Synuclein is localized to mitochondria-associated ER membranes. *J Neurosci* 34:249–259. <https://doi.org/10.1523/JNEUROSCI.2507-13.2014>
37. Hafner A-S, Donlin-Asp PG, Leitch B, Herzog E, Schuman EM (2019) Local protein synthesis is a ubiquitous feature of neuronal pre- and postsynaptic compartments. *Science*. <https://doi.org/10.1126/science.aau3644>
38. Hashimoto K, Ishima T (2011) Neurite outgrowth mediated by translation elongation factor eEF1A1: a target for antiplatelet agent cilostazol. *PLoS ONE* 6:e17431. <https://doi.org/10.1371/journal.pone.0017431>
39. Herzog E, Nadrigny F, Silm K, Biesemann C, Helling I, Bersot T, Steffens H, Schwartzmann R, Nagerl UV, El Mestikawy S, Rhee J, Kirchhoff F, Brose N (2011) In vivo imaging of intersynaptic vesicle exchange using VGLUT1 Venus knock-in mice. *J Neurosci* 31:15544–15559. <https://doi.org/10.1523/JNEUROSCI.2073-11.2011>
40. Hosp F, Mann M (2017) A primer on concepts and applications of proteomics in neuroscience. *Neuron* 96:558–571. <https://doi.org/10.1016/j.neuron.2017.09.025>

41. Hu Q, Wang G (2016) Mitochondrial dysfunction in Parkinson's disease. *Transl Neurodegener* 5:14. <https://doi.org/10.1186/s40035-016-0060-6>
42. Huang DW, Sherman BT, Lempicki RA (2008) Systematic and integrative analysis of large gene lists using DAVID bioinformatics resources. *Nat Protoc* 4:44–57. <https://doi.org/10.1038/nprot.2008.211>
43. Huang DW, Sherman BT, Lempicki RA (2009) Bioinformatics enrichment tools: paths toward the comprehensive functional analysis of large gene lists. *Nucleic Acids Res* 37:1–13. <https://doi.org/10.1093/nar/gkn923>
44. Iketani M, Iizuka A, Sengoku K, Kurihara Y, Nakamura F, Sasaki Y, Sato Y, Yamane M, Matsushita M, Nairn AC, Takamatsu K, Goshima Y, Takei K (2013) Regulation of neurite outgrowth mediated by localized phosphorylation of protein translational factor eEF2 in growth cones. *Dev Neurobiol* 73:230–246. <https://doi.org/10.1002/dneu.22058>
45. Kilkenny C, Browne WJ, Cuthill IC, Emerson M, Altman DG (2012) Improving bioscience research reporting: the ARRIVE guidelines for reporting animal research. *Osteoarthritis Cartil* 20:256–260
46. Liu G, Tang J, Edmonds BT, Murray J, Levin S, Condeelis J (1996) F-actin sequesters elongation factor 1alpha from interaction with aminoacyl-tRNA in a pH-dependent reaction. *J Cell Biol* 135:953–963
47. Liu G, Wang P, Li X, Li Y, Xu S, Uéda K, Chan P, Yu S (2013) Alpha-synuclein promotes early neurite outgrowth in cultured primary neurons. *J Neural Transm* 120:1331–1343. <https://doi.org/10.1007/s00702-013-0999-8>
48. Logan T, Bendor J, Toupin C, Thorn K, Edwards RH (2017) α -Synuclein promotes dilation of the exocytotic fusion pore. *Nat Neurosci* 20:681–689. <https://doi.org/10.1038/nn.4529>
49. Lotharius J, Brundin P (2002) Pathogenesis of Parkinson's disease: dopamine, vesicles and alpha-synuclein. *Nat Rev Neurosci* 3:932–942. <https://doi.org/10.1038/nrn983>
50. Luquet E, Biesemann C, Munier A, Herzog E (2017) Purification of synaptosome populations using fluorescence-activated synaptosome sorting. *Methods Mol Biol Clifton NJ* 1538:121–134. https://doi.org/10.1007/978-1-4939-6688-2_10
51. Ma T, Trinh MA, Wexler AJ, Bourbon C, Gatti E, Pierre P, Cavener DR, Klann E (2013) Suppression of eIF2 α kinases alleviates Alzheimer's disease-related plasticity and memory deficits. *Nat Neurosci* 16:1299–1305. <https://doi.org/10.1038/nn.3486>
52. Masliah E (2000) Dopaminergic loss and inclusion body formation in α -synuclein mice: implications for neurodegenerative disorders. *Science* 287:1265–1269. <https://doi.org/10.1126/science.287.5456.1265>
53. Mateyak MK, Kinzy TG (2010) eEF1A: thinking outside the ribosome. *J Biol Chem* 285:21209–21213. <https://doi.org/10.1074/jbc.R110.113795>
54. McClatchy DB, Fang G, Levey AI (2006) Elongation factor 1A family regulates the recycling of the M4 muscarinic acetylcholine receptor. *Neurochem Res* 31:975–988. <https://doi.org/10.1007/s11064-006-9103-1>
55. McInnes J, Wierda K, Snellinx A, Bounti L, Wang Y-C, Stancu I-C, Apóstolo N, Gevaert K, Dewachter I, Spires-Jones TL, De Strooper B, De Wit J, Zhou L, Verstreken P (2018) Synaptogyrin-3 mediates presynaptic dysfunction induced by Tau. *Neuron* 97:823–835.e8. <https://doi.org/10.1016/j.neuron.2018.01.022>
56. Moreno JA, Radford H, Peretti D, Steinert JR, Verity N, Martin MG, Halliday M, Morgan J, Dinsdale D, Ortori CA, Barrett DA, Tsaytler P, Bertolotti A, Willis AE, Bushell M, Mallucci GR (2012) Sustained translational repression by eIF2 α -P mediates prion neurodegeneration. *Nature* 485:507–511. <https://doi.org/10.1038/nature11058>
57. Nakamura K, Nemani VM, Azarbal F, Skibinski G, Levy JM, Egami K, Munishkina L, Zhang J, Gardner B, Wakabayashi J, Sesaki H, Cheng Y, Finkbeiner S, Nussbaum RL, Masliah E, Edwards RH (2011) Direct membrane association drives mitochondrial fission by the Parkinson disease-associated protein alpha-synuclein. *J Biol Chem* 286:20710–20726. <https://doi.org/10.1074/jbc.M110.213538>
58. Nakayama K, Suzuki Y, Yazawa I (2012) Binding of neuronal α -synuclein to β -III tubulin and accumulation in a model of multiple system atrophy. *Biochem Biophys Res Commun* 417:1170–1175. <https://doi.org/10.1016/j.bbrc.2011.12.092>
59. Nemani VM, Lu W, Berge V, Nakamura K, Onoa B, Lee MK, Chaudhry FA, Nicoll RA, Edwards RH (2010) Increased expression of α -synuclein reduces neurotransmitter release by inhibiting synaptic vesicle reclustering after endocytosis. *Neuron* 65:66–79. <https://doi.org/10.1016/j.neuron.2009.12.023>
60. Park J, Park Y, Ryu I, Choi M-H, Lee HJ, Oh N, Kim K, Kim KM, Choe J, Lee C, Baik J-H, Kim YK (2017) Misfolded polypeptides are selectively recognized and transported toward aggresomes by a CED complex. *Nat Commun* 8:15730. <https://doi.org/10.1038/ncomms15730>
61. Petroulakis E, Wang E (2002) Nerve growth factor specifically stimulates translation of eukaryotic elongation factor 1A-1 (eEF1A-1) mRNA by recruitment to polyribosomes in PC12 cells. *J Biol Chem* 277:18718–18727. <https://doi.org/10.1074/jbc.M111782200>
62. Picconi B, Piccoli G, Calabresi P (2012) Synaptic dysfunction in Parkinson's disease. *Adv Exp Med Biol* 970:553–572. https://doi.org/10.1007/978-3-7091-0932-8_24
63. Plotegher N, Kumar D, Tessari I, Brucale M, Munari F, Tosatto L, Belluzzi E, Greggio E, Bisaglia M, Capaldi S, Aioanei D, Mammi S, Monaco HL, Samo B, Bubacco L (2014) The chaperone-like protein 14-3-3 η interacts with human α -synuclein aggregation intermediates rerouting the amyloidogenic pathway and reducing α -synuclein cellular toxicity. *Hum Mol Genet* 23:5615–5629. <https://doi.org/10.1093/hmg/ddu275>
64. Prots I, Veber V, Brey S, Campioni S, Buder K, Riek R, Bohm KJ, Winner B (2013) Synuclein oligomers impair neuronal microtubule-kinesin interplay. *J Biol Chem* 288:21742–21754. <https://doi.org/10.1074/jbc.M113.451815>
65. Ruest L-B, Marcotte R, Wang E (2002) Peptide elongation factor eEF1A-2/S1 expression in cultured differentiated myotubes and its protective effect against caspase-3-mediated apoptosis. *J Biol Chem* 277:5418–5425. <https://doi.org/10.1074/jbc.M110685200>
66. Schreiner D, Savas JN, Herzog E, Brose N, de Wit J (2017) Synapse biology in the 'circuit-age'-paths toward molecular connectomics. *Curr Opin Neurobiol* 42:102–110. <https://doi.org/10.1016/j.conb.2016.12.004>
67. Scott D, Roy S (2012) α -Synuclein inhibits intersynaptic vesicle mobility and maintains recycling-pool homeostasis. *J Neurosci* 32:10129–10135. <https://doi.org/10.1523/JNEUROSCI.0535-12.2012>
68. Sharma K, Schmitt S, Bergner CG, Tyanova S, Kannaiyan N, Manrique-Hoyos N, Kongi K, Cantuti L, Hanisch U-K, Philips M-A, Rossner MJ, Mann M, Simons M (2015) Cell type- and brain region-resolved mouse brain proteome. *Nat Neurosci* 18:1819–1831. <https://doi.org/10.1038/nn.4160>
69. Shigeoka T, Jung H, Jung J, Turner-Bridger B, Ohk J, Lin JQ, Amieux PS, Holt CE (2016) Dynamic axonal translation in developing and mature visual circuits. *Cell* 166:181–192. <https://doi.org/10.1016/j.cell.2016.05.029>
70. Spillantini MG, Schmidt ML, Lee VM, Trojanowski JQ, Jakes R, Goedert M (1997) Alpha-synuclein in Lewy bodies. *Nature* 388:839–840. <https://doi.org/10.1038/42166>
71. Suzuki Y, Jin C, Iwase T, Yazawa I (2014) III Tubulin fragments inhibit—synuclein accumulation in models of multiple system

- atrophy. *J Biol Chem* 289:24374–24382. <https://doi.org/10.1074/jbc.M114.557215>
72. Taylor AM, Berchtold NC, Perreau VM, Tu CH, Li Jeon N, Cotman CW (2009) Axonal mRNA in uninjured and regenerating cortical mammalian axons. *J Neurosci* 29:4697–4707. <https://doi.org/10.1523/JNEUROSCI.6130-08.2009>
73. Terry RD, Masliah E, Salmon DP, Butters N, DeTeresa R, Hill R, Hansen LA, Katzman R (1991) Physical basis of cognitive alterations in Alzheimer's disease: synapse loss is the major correlate of cognitive impairment. *Ann Neurol* 30:572–580. <https://doi.org/10.1002/ana.410300410>
74. Tsokas P, Grace EA, Chan P, Ma T, Sealfon SC, Iyengar R, Landau EM, Blitzer RD (2005) Local protein synthesis mediates a rapid increase in dendritic elongation factor 1A after induction of late long-term potentiation. *J Neurosci* 25:5833–5843. <https://doi.org/10.1523/JNEUROSCI.0599-05.2005>
75. Vargas KJ, Makani S, Davis T, Westphal CH, Castillo PE, Chandra SS (2014) Synucleins regulate the kinetics of synaptic vesicle endocytosis. *J Neurosci* 34:9364–9376. <https://doi.org/10.1523/JNEUROSCI.4787-13.2014>
76. Vizcaíno JA, Csordas A, del-Toro N, Dians JA, Griss J, Lavidas I, Mayer G, Perez-Riverol Y, Reisinger F, Ternent T, Xu Q-W, Wang R, Hermjakob H (2016) 2016 update of the PRIDE database and its related tools. *Nucleic Acids Res* 44:D447–D456. <https://doi.org/10.1093/nar/gkv1145>
77. Walker L, Stefanis L, Attems J (2019) Clinical and neuropathological differences between Parkinson's disease, Parkinson's disease dementia and dementia with Lewy bodies—current issues and future directions. *J Neurochem*. <https://doi.org/10.1111/jnc.14698>
78. Wang X, Huang T, Bu G, Xu H (2014) Dysregulation of protein trafficking in neurodegeneration. *Mol Neurodegener* 9:31
79. Whittaker VP, Michaelson I, Kirkland RJA (1964) The separation of synaptic vesicles from nerve-ending particles (synaptosomes¹). *Biochem J* 90:293
80. Wong YC, Krainc D (2017) α -synuclein toxicity in neurodegeneration: mechanism and therapeutic strategies. *Nat Med* 23:1–13. <https://doi.org/10.1038/nm.4269>
81. Xu J, Wu X-S, Sheng J, Zhang Z, Yue H-Y, Sun L, Sgobio C, Lin X, Peng S, Jin Y, Gan L, Cai H, Wu L-G (2016) α -Synuclein mutation inhibits endocytosis at mammalian central nerve terminals. *J Neurosci* 36:4408–4414. <https://doi.org/10.1523/JNEUROSCI.3627-15.2016>
82. Yang F, Demma M, Warren V, Dharmawardhane S, Condeelis J (1990) Identification of an actin-binding protein from dictyostelium as elongation factor 1a. *Nature* 347:494–496. <https://doi.org/10.1038/347494a0>

Publisher's Note Springer Nature remains neutral with regard to jurisdictional claims in published maps and institutional affiliations.